Mon. Not. R. Astron. Soc. **420,** 2518–2525 (2012) doi:10.1111/j.1365-2966.2011.20216.x

The environment of weak emission-line quasars

M. Nikołajuk[1,2]★ and R. Walter[1]★

[1]*ISDC Data Centre for Astrophysics, Chemin d'Ecogia 16, CH-1290 Versoix, Switzerland*
[2]*Faculty of Physics, University of Bialystok, Lipowa 41, PL-15424 Białystok, Poland*

Accepted 2011 November 16. Received 2011 October 27; in original form 2011 July 26

ABSTRACT

The nature of weak emission-line quasars (WLQs) is probed by comparing the Baldwin effect (BEff) in WLQs and normal quasars [quasi-stellar objects (QSOs)]. We selected 81 high-redshift ($z > 2.2$) and two intermediate-redshift ($z = 1.66$ and 1.89) WLQs. Their rest-frame equivalent widths (EWs) of the C IV emission line and their Eddington ratio were obtained from the Sloan Digital Sky Survey Data Release 7 (SDSS DR7) quasar catalogue or from Diamond-Stanic et al. We compare the parameters of WLQs with those of 81 normal quasars from Bright Quasar Survey and 155 radio-quiet and radio-intermediate quasars detected by SDSS and *Chandra*. The influence of the Eddington ratio, $L_{\rm Bol}/L_{\rm Edd}$, and the X-ray to optical luminosity ratio, $\alpha_{\rm ox}$, on the BEff is analysed. We find that WLQs follow a different relationship on the EW(C IV)–$L_{\rm Bol}/L_{\rm Edd}$ plane than normal quasars. This relationship disagrees with the super-Eddington hypothesis. The weakness/absence of emission lines in WLQs does not seem to be caused by their extremely soft ionizing continuum but by low covering factor ($\Omega/4\pi$) of their broad-line region. Comparison of emission-line intensities indicates that the ratios of high-ionization line and low-ionization line regions (i.e. $\Omega_{\rm HIL}/\Omega_{\rm LIL}$) are lower in WLQs than in normal QSOs. The covering factors of the regions producing C IV and Lyα emission lines are similar in both WLQs and QSOs.

Key words: galaxies: active – quasars: emission lines – ultraviolet: galaxies – X-rays: galaxies.

1 INTRODUCTION

A negative correlation between the broad emission-line equivalent width (EW) and the luminosity in active galactic nuclei (AGNs) was discovered by Baldwin (1977) for the C IV λ1549 line. Similar correlations (the Baldwin effect, hereafter BEff) are also observed for other lines such as Lyα λ1216, Si IV+O IV λ1400, He II λλ1640, 4686, C III] λ1909, Mg II λ2800, Fe lines in the ultraviolet (UV) and optical bands, and the Balmer lines produced in the broad-line region (BLR; see e.g. Kinney, Rivolo & Koratkar 1990; Zamorani et al. 1992; Green, Forster & Kuraszkiewicz 2001; Kuraszkiewicz et al. 2002; Shang et al. 2003). This effect was also observed in single objects (e.g. NGC 5548 and 4151), when the intrinsic ionizing continuum is varying (Kinney et al. 1990; Pogge & Peterson 1992; Gilbert & Peterson 2003; Kong et al. 2006). At least some of the emission lines produced in the narrow-line region display a BEff as well (e.g. Boroson & Green 1992; Dietrich et al. 2002; Keremedjiev, Hao & Charmandaris 2009). Furthermore, an X-ray BEff in the iron K lines was detected by Iwasawa & Taniguchi (1993) and analysed by e.g. Jiang, Wang & Wang (2006) and Bianchi et al. (2007).

★E-mail: Marek.Nikolajuk@unige.ch; mrk@alpha.uwb.edu.pl (MN); Roland.Walter@unige.ch (RW)

Several physical explanations have been proposed to explain the BEff. The most supported hypothesis is that the more luminous objects have softer UV/X-ray spectra reducing ionization and photoelectric heating in the BLR gas. Ipso facto, the EWs of emission lines are reduced at higher luminosity with the strongest effect for high-ionization lines (HILs; see Korista, Baldwin & Ferland 1998; Shields 2007, for a review of the BEff). Fundamental parameters such as the Eddington ratio (Bachev et al. 2004; Baskin & Laor 2004; Warner, Hamann & Dietrich 2004; Zhou & Wang 2005; Xu et al. 2008; Dong et al. 2009), the black hole mass (Netzer, Laor & Gondhalekar 1992; Shields 2007) or metallicity (Warner et al. 2004) have also been suggested as the driver of the BEff.

The discovery of weak emission-line quasars (WLQs), i.e. sources with abnormally low broad emission lines [e.g. EW(Lyα)$_{\rm WLQ}$ < 15.4 Å; Diamond-Stanic et al. 2009], provides new constraints on the driving mechanism of the BEff. The first WLQ object PG 1407+265 (with redshift $z = 0.94$) was discovered by McDowell et al. (1995). However, up to 2009 only about 20 WLQs were known. They mostly lie at high redshifts ($z > 2.2$), like SDSS J153259.96−003944.1 (Fan et al. 1999; the first high-z WLQ, with $z = 4.62$), and were found in the Sloan Digital Sky Survey (SDSS) (Anderson et al. 2001; Schneider et al. 2003, 2005, 2007; Collinge et al. 2005; Fan et al. 2006; Shemmer et al. 2009). Diamond-Stanic et al. (2009) recently discovered 65 new high-z WLQs, which may suggest that there is a deficit of weak-line quasars below $z < 2$. However, Plotkin et al. (2010a,b) pointed out that more intermediate- and low-redshift WLQ may also exist.

There are no generally accepted explanations for the weakness or even absence of emission lines in WLQ. Several hypotheses were suggested by McDowell et al. (1995). Relativistic beaming in WLQ is not favoured as weak-line quasars, in contrast to BL Lacs, are radio-quiet objects,[1] show no variability or strong polarization. Moreover, the radio spectral slopes, connecting $\lambda \sim 6$ cm with $\sim$20 cm, are significantly steeper in radio-detected WLQs than the typical slopes for BL Lac, $\alpha_r \sim 0.3$ (Shemmer et al. 2006, 2009; Diamond-Stanic et al. 2009; Plotkin et al. 2010a). The idea that WLQs could be broad absorption line (BAL) quasars also meets difficulties. Generally, they do not show broad absorption features and are classified as non-BAL objects (Diamond-Stanic et al. 2009; Shen et al. 2011).

Two leading hypotheses to explain the weakness of emission lines in WLQ have been suggested.

(1) The first one is related to the BEff. Weak emission lines may be a consequence of a very soft ionizing continuum and of a relative deficiency of high-energy UV/X-ray photons.[2] Leighly et al. (2007a), based on observation of PHL 1811, have claimed that its very soft spectral energy distribution (SED; the photon index $\alpha_{ox} = 2.3 \pm 0.1$)[3] is related to its super-Eddington nature (the estimated L_{Bol}/L_{Edd} lies in the range 0.9–1.6). However, it is worth noting that the observed UV/optical part of the continuum in WLQs looks like those of normal quasars. Richards et al. (2003) have analysed the spectra of 4576 SDSS quasars and they found that the spectral indices, α_ν (where $f_\nu \propto \nu^{\alpha_\nu}$), lie in a wide range, with mean values from −0.25 to −0.76 (see their composite nos. 1–4). The spectral indices in WLQs also span the same interval with a median values of $\alpha_\nu = -0.52$ (Diamond-Stanic et al. 2009; Plotkin et al. 2010a). Those values mean that, generally, the observed UV SED in WLQ is not particularly soft. However, these objects may still emit more vigorously in the unobserved far-UV (FUV) band. Recently, Wu et al. (2011) found a small population of X-ray weak quasars, suggesting that these PHL 1811 analogues possess the shielding gas with large covering factor. This gas absorbs almost all soft X-ray continuum to prevent illumination of BLR by this radiation. As a result, weak emission lines are produced although a face-on observer sees the normal X-ray continuum.

(2) The second hypothesis suggests that WLQs are normal quasars with typical metallicities, ionizing continua and ionization parameters, however, with an underdeveloped BLR perhaps because of a freshly launched accretion disc wind (Hryniewicz et al. 2010). The weakness/absence of emission lines in this case is caused by a low BLR covering factor or a deficit of line-emitting gas in the BLR (Shemmer et al. 2010).

[1] The radio loudness parameter R is defined as the ratio of the rest-frame 6 cm to 2500 Å flux densities (see Jiang et al. 2007; Shen et al. 2011). Among 70 radio-detected WLQs analysed by Diamond-Stanic et al. (2009), 81 per cent of sources have $R \leq 25$ and only 7 per cent are radio-loud WLQs, i.e. $R > 100$.

[2] 'The very soft ionizing continuum' means that a continuum in the far-UV band is characterized by a steep spectrum. We use the X-ray to optical luminosity ratio, α_{ox} (see definition below). For typical quasar α_{ox} is equal to −1.50 (Laor et al. 1997), and for the most luminous quasars with redshift 1.5–4.5 the mean α_{ox} equals −1.80 (Just et al. 2007). We adopt $\alpha_{ox} < -2.0$ as a definition of a very soft spectrum.

[3] $\alpha_{ox} = 0.3838 \log\,[L_\nu(2\,\mathrm{keV})/L_\nu(2500\,\text{Å})]$ (e.g. Avni & Tananbaum 1982; Strateva et al. 2005; Gibson, Brandt & Schneider 2008).

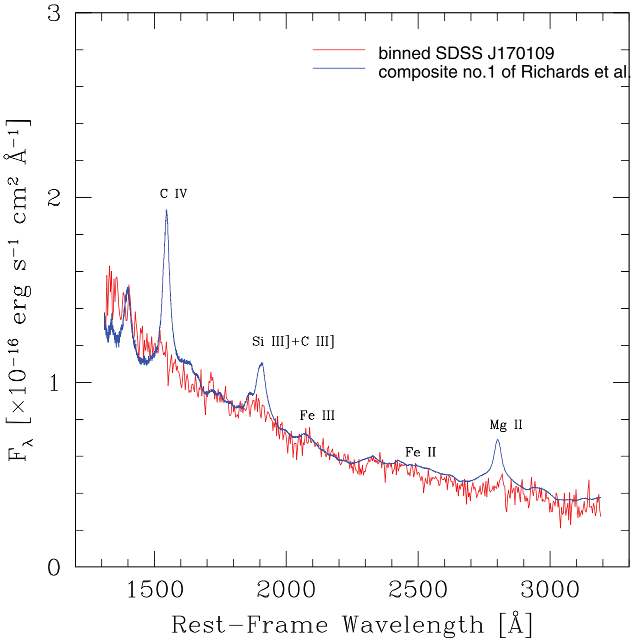

Figure 1. The rest-frame spectrum of SDSS J170109 binned and corrected for Galactic reddening using the Cardelli, Clayton & Mathis (1989) relationship. For comparison, the Richards et al. (2003) composite spectrum (no. 1) is shown.

In this paper, we analyse both hypotheses: softness of ionizing continuum and underdevelopment of BLR. In Section 2, we describe the sample of quasars that was used. Section 3 is devoted to the comparison of the observed properties of WLQ and quasi-stellar object (QSO) that we discuss in Section 4. The conclusions are presented in Section 5. We assume that $H_0 = 70\,\mathrm{km\,s^{-1}\,Mpc^{-1}}$, $\Omega_m = 0.3$ and $\Omega_\Lambda = 0.7$.

2 THE WLQ SAMPLE

The sample of WLQs consists of 81 high-redshift ($z > 2.2$) and high-bolometric luminosity ($\log L_{Bol} = 46.5$–47.9) sources classified by Anderson et al. (2001), Collinge et al. (2005), Schneider et al. (2007), Shemmer et al. (2009), Diamond-Stanic et al. (2009) and Plotkin et al. (2010a), extended by two quasars SDSS J094533.98+100950.1 (hereafter SDSS J094534) and SDSS J170108.89+395443.0 (hereafter SDSS J170109). Both sources lie at intermediate-redshift distances with z of 1.66 and 1.89, respectively.

A spectrum of SDSS J094534 was analysed extensively by Hryniewicz et al. (2010). The second source (see its spectrum in Fig. 1) was retrieved serendipitously by us in the SDSS Data Release 7 (DR7) quasar catalogue (Shen et al. 2011). We classified it as WLQ because (1) the EWs of C IV and Mg II measured at the rest frame are small [i.e. EW(C IV) = 2.09 ± 1.83 Å, EW(Mg II) = 9.41 ± 2.03 Å; Shen et al. 2011], (2) this quasar is radio intermediate as a dozen WLQ sources (rest-frame $f_{6cm}/f_{2500} = 45.3$; Shen et al. 2011) and (3) the UV continuum of SDSS J170109 can be fitted as a power law ($f_\nu \propto \nu^{\alpha_\nu}$) with a spectral index $\alpha_\nu = -0.23 \pm 0.03$[4] identical within errors to that of the quasar composite from Richards et al. (2003). This value also differs from the mean spectral index

[4] This value is equivalent to $\alpha_\lambda = -1.77$, where $f_\lambda \propto \lambda^{\alpha_\lambda}$.

calculated for BL Lac candidates for which we have $\langle \alpha_\nu \rangle = -1.15$ (Plotkin et al. 2010a).

All sources were detected by the SDSS. In our analysis, we are using the EWs of emission lines measured in the rest frame, fluxes of those lines, masses of the supermassive black holes, $M_{\rm BH}$, accretion rates in the Eddington units, $L_{\rm Bol}/L_{\rm Edd}$, and the spectral indices, $\alpha_{\rm ox}$. Almost all but $\alpha_{\rm ox}$ values were found in the SDSS DR7 quasar catalogue (Shen et al. 2011). Shen et al. (2011) point out that estimated EW(C IV) are encumbered with large error when the signal-to-noise ratio of the observed WLQ spectrum is lower than 5 (see their fig. 8). Therefore, in these cases we use EW values estimated by Diamond-Stanic et al. (2009), which for all sources but two have EW(C IV) $>5\sigma$. In other cases, we use upper limits taken from the quasar catalogue or calculate them (see Table 1). The spectral indices, $\alpha_{\rm ox}$, of WLQs were taken from Shemmer et al. (2006, 2009). All those values originate from the *Chandra* observations. Additionally, we checked the *Chandra* Multiwavelength Project Catalogue (Green et al. 2009). We cross-correlated this catalogue with SDSS DR7. No new WLQs but SDSS J170109 were found. Its $\alpha_{\rm ox}$ is equal to -1.29.

3 COMPARISON OF WLQs WITH NORMAL QUASARS

Our aim is to compare the BEff observed in weak WLQs to that observed in normal type 1 quasars. Fig. 2 displays the EW of the C IV emission line against the dimensionless accretion rates for different types of quasars. This figure includes 81 quasars from the Bright Quasar Survey (BQS) with redshifts $z < 0.5$ and bolometric values $\log L_{\rm Bol} = 44.2$–46.9 analysed by Boroson & Green (1992). Baskin & Laor (2004) estimated their EW(C IV) and $L_{\rm Bol}/L_{\rm Edd}$. Dashed line represents the best linear fit to their data (Baskin & Laor 2004, 2005). The triangles show 76 WLQs for which the EW and the accretion ratios were calculated by Shen et al. (2011) or Diamond-Stanic et al. (2009). We must note here that in the papers of both Baskin & Laor and Shen et al., the methods to estimate $L_{\rm Bol}/L_{\rm Edd}$ are similar. Both calculated the bolometric luminosity using the relationship $L_{\rm Bol} = BC_\lambda \times L_{\lambda,\rm cont}$, where $L_{\lambda,\rm cont}$ is the continuum luminosity measured at wavelength λ and BC_λ is the appropriate bolometric correction factor. Both methods estimate the Eddington luminosity, $L_{\rm Edd} \propto M_{\rm BH}$, using the scaling method in order to calculate the black hole mass in AGN, i.e. $M_{\rm BH} \propto L^{\rm b}_{\lambda,\rm cont}\,{\rm FWHM}^2({\rm ion})$. In this equation, FWHM stands for the full width at half-maximum of ion which produces the emission line. BQS quasars and high-z WLQs lie at different distances; therefore, Baskin & Laor and Shen et al. used observations of different emission lines and continuum luminosities to calculate $M_{\rm BH}$. Baskin & Laor (2004) used FWHM of Hβ line, $L_{\lambda,\rm cont}$ measured at 5100 Å in the rest frame of quasar and $b = 0.50$ (see equation 3 in Laor 1998). The authors used Hβ emission line to estimate $L_{\rm Bol}/L_{\rm Edd}$ because many scientists suggest non-virialized character of C IV (e.g. Risaliti, Young & Elvis 2009; Fine et al. 2010; Richards et al. 2011). However, high-z WLQs have redshifts higher than 2.2. Therefore, Shen et al. (2011) used C IV line and continuum luminosity observed at 1350 Å. They used the relationship determined by Vestergaard & Peterson (2006) between $M_{\rm BH}$, FWHM and $L_{\lambda,\rm cont}$ for which $b = 0.53$. Baskin & Laor (2004) found an anticorrelation between EW(C IV) and $L_{\rm Bol}/L_{\rm Edd}$. However, if one calculates Eddington ratios based on C IV emission lines, this relationship is much weaker than the correlation with the $L_{\rm Bol}/L_{\rm Edd}$ estimated based on Hβ (Baskin & Laor 2005).

In this paper, we analyse 83 weak WLQs; however, in Fig. 2 only 76 of them have C IV emission line strong enough to determine their $L_{\rm Bol}/L_{\rm Edd}$ (see Table 1). The EWs of the remaining WLQs are lower than ∼3 or 7 Å for sources with stronger or weaker UV fluxes, respectively. It is worth noting that one object of the BQS lies in the region dominated by WLQ. This is the radio-quiet quasar (PG 0043+039, $z = 0.384$) with EW(C IV) = 5.4 ± 3.7 Å (Baskin & Laor 2004). Its Hβ emission line is strong with EW = 92 Å, whereas O [III] λ5007 and He II λ4686 are weak, with EWs equal to 1 and 0 Å, respectively (Boroson & Green 1992).

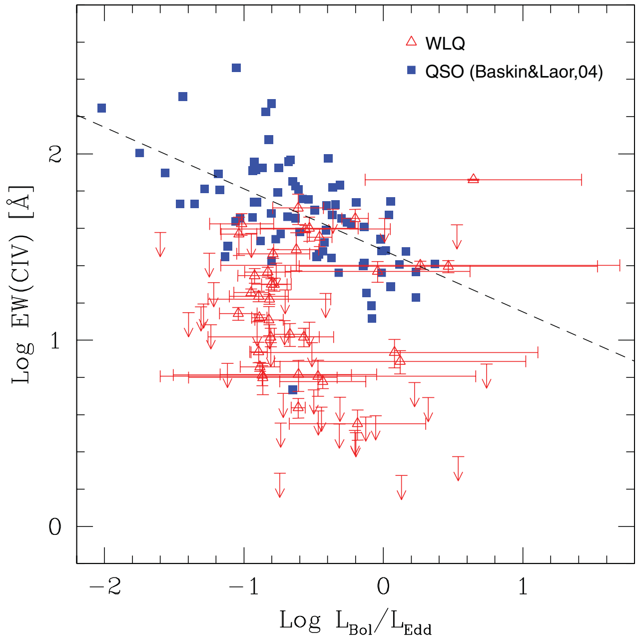

Figure 2. EW of C IV measured at the rest frame plotted against accretion ratio. Filled blue squares show 81 BQS quasars analysed by Baskin & Laor (2004). Filled red triangles and upper limits refer to 76 WLQs taken from Shen et al. (2011) or Diamond-Stanic et al. (2009). Points with error bars refer to objects with a significance of EW higher than 5σ. Otherwise, upper limits are shown. Dashed line is the best linear fit to BQS quasars (Baskin & Laor 2004, 2005).

In contrast to PG 0043+039, several (17 from 76) WLQs have large EWs of C IV line and behave like normal type 1 quasars. Their median distance from the linear fit of Baskin & Laor is only 2.3σ when for 'genuine' WLQs it is larger ($>7\sigma$). We must mention that Shemmer et al. (2009) decided to use EW(C IV) $\lesssim 10$ Å as a hallmark of WLQs. However, Diamond-Stanic et al. (2009) decided to use EW of Lyα+N V blend as these lines are better seen in distant weak-line quasars. Therefore, we kept this definition [i.e. EW(Lyα+N V) < 15.4 Å] as a rule for our study. We suggest that the weakness of the EW(Lyα+N V) in the sources with prominent C IV emission lines is caused by strong absorption of the Lyα region and that they are, in fact, normal quasars.

The best linear fit to BQS quasars sample (seen in Fig. 2) suggests that WLQs follow a different relationship than normal quasars between EW and the accretion ratio. The errors of those quantities for WLQ are large and, unfortunately, we cannot fit a correlation to them. However, in order to statistically quantify the hypothesis about different relations, we compare the reduced χ^2 ($\tilde{\chi}^2$) in the cases of BQS and WLQ. We divide our WLQ objects into two subsets. The first one consists of all 76 weak WLQs. In the second case, we exclude all the upper limits on EW(C IV) from our subset. We also assume that the obtained fit parameters for normal quasars are also the same for WLQs. The estimated reduced χ^2 is 27.7 in the case of BQS quasars. This value is significantly larger than 1.

Table 1. The sample of weak WLQs.

Name	$z_{\rm SDSS}$	EW(C IV) (Å)	Ref.	$\log M_{\rm BH}$ ($M_\odot$)	$\alpha_{\rm ox}$	Ref.	$\log L_{\rm Bol}/L_{\rm Edd}$
SDSS 010802.90−010946.1	3.330	≤15.1		10.243 ± 0.390			−1.308 ± 0.390
SDSS 025646.56+003858.3	3.473	6.3 ± 1.2	(1)	9.968 ± 0.532			−0.865 ± 0.532
SDSS 031712.23−075850.3	2.695	≤1.0	(2)		−1.58	(3)	
SDSS 080523.32+214921.1	3.463	23.4 ± 3.0		9.107 ± 0.662			−0.042 ± 0.662
SDSS 080906.87+172955.1	2.953	3.6 ± 0.7		9.509 ± 0.489			−0.185 ± 0.489
SDSS 082059.34+561021.9	3.636	31.6 ± 4.7		9.376 ± 0.089			−0.457 ± 0.090
SDSS 082638.59+515233.2	2.850	4.3 ± 0.5		10.369 ± 0.050			−0.610 ± 0.050
SDSS 083122.57+404623.3	4.885	≤10.5		9.727 ± 0.621			−0.311 ± 0.621
SDSS 083304.73+415331.3	2.329	≤4.2		9.107 ± 0.471			−0.467 ± 0.471
SDSS 083330.56+233909.1	2.417	≤5.4		9.199 ± 0.464			−0.499 ± 0.465
SDSS 084249.03+235204.7	3.316	≤9.7		9.422 ± 0.247			−0.512 ± 0.247
SDSS 084424.24+124546.5	2.505	≤3.5		9.592 ± 0.197			−0.315 ± 0.197
SDSS 084434.15+224305.2	3.117	42.1 ± 5.6		9.860 ± 0.229			−1.016 ± 0.229
SDSS 090703.91+410748.3	2.672	≤1.9		8.727 ± 0.101			0.129 ± 0.102
SDSS 091738.90+082053.9	3.252	18.0 ± 0.8	(1)	9.853 ± 0.124			−0.948 ± 0.125
SDSS 092312.75+174452.8	2.260	≤7.5		9.960 ± 0.414			−1.117 ± 0.414
SDSS 093306.88+332556.6	4.560	≤37.3		10.073 ± 0.744			−0.946 ± 0.744
SDSS 094533.98+100950.1	1.661	≤4.0		9.786 ± 0.036			−0.753 ± 0.036
SDSS 095108.76+314705.8	3.032	≤12.1		9.770 ± 0.507			−1.237 ± 0.508
SDSS 101204.04+531331.7	2.990	≤3.7		9.510 ± 0.398	−1.49	(3)	−0.736 ± 0.399
SDSS 101849.78+271914.9	2.603	≤4.9		8.331 ± 0.956			0.322 ± 0.956
SDSS 102609.92+253651.2	2.317	≤3.3		8.998 ± 0.515			−0.203 ± 0.515
SDSS 102949.80+605731.7	3.190	37.1 ± 8.6		9.624 ± 0.128			−1.036 ± 0.131
SDSS 103240.54+501211.0	3.874	≤12.5		9.779 ± 0.140			−0.531 ± 0.142
SDSS 104650.29+295206.8	4.266	≤37.8		10.530 ± 0.317			−1.599 ± 0.321
SDSS 105049.27+441144.7	4.320	≤9.7		10.039 ± 0.573			−0.808 ± 0.574
SDSS 111642.81+420324.9	2.526	≤3.2		9.142 ± 1.604			−0.198 ± 1.604
SDSS 113354.89+022420.9	3.990	16.1 ± 2.1		10.014 ± 0.092			−0.782 ± 0.093
SDSS 113729.42+375224.2	4.166	≤7.4		8.193 ± 1.069			0.740 ± 1.069
SDSS 113747.64+391941.5	2.395	≤5.9		8.507 ± 1.167			0.224 ± 1.167
SDSS 114153.33+021924.3	3.480	≤1.0	(2)		−1.54	(3)	
SDSS 114412.76+315800.8	3.235	6.8 ± 1.0		10.128 ± 0.143			−0.884 ± 0.143
SDSS 114958.53+375115.0	4.315	≤41.5		8.310 ± 1.875			0.527 ± 1.876
SDSS 115254.96+150707.7	3.328	10.4 ± 1.2	(1)	10.080 ± 0.450			−0.807 ± 0.450
SDSS 115308.45+374232.1	3.028	17.2 ± 1.1	(1)	9.690 ± 0.211			−0.894 ± 0.212
SDSS 115906.52+133737.7	3.984	13.0 ± 1.2		10.664 ± 0.055			−0.889 ± 0.055
SDSS 115933.53+054141.6	3.286	29.1 ± 1.6	(1)	9.425 ± 0.262			−0.791 ± 0.263
SDSS 115959.71+410152.9	2.788	8.7 ± 1.1		10.427 ± 0.063			−0.895 ± 0.063
SDSS 120059.68+400913.1	3.366	72.6 ± 0.5		8.177 ± 0.775			0.645 ± 0.776
SDSS 121221.56+534127.8	3.097	≤3.0			−1.93	(3)	
SDSS 121812.39+444544.5	4.518	≤20.4		10.314 ± 0.621			−1.216 ± 0.622
SDSS 122021.39+092135.8	4.110	25.2 ± 1.3	(1)	8.971 ± 1.429			0.264 ± 1.430
SDSS 122359.35+112800.0	4.120	≤37.6		9.781 ± 0.161			−0.624 ± 0.163
SDSS 122445.26+375921.3	4.315	≤18.9		9.314 ± 1.205			−0.414 ± 1.207
SDSS 123116.08+411337.3	3.838	≤12.1		9.732 ± 0.458			−0.816 ± 0.458
SDSS 123132.37+013814.0	3.229	≤1.9		9.997 ± 0.670	−1.37	(3)	−0.742 ± 0.670
SDSS 123315.94+313218.4	3.222	6.4 ± 1.4	(1)	9.163 ± 1.131			−0.469 ± 1.131
SDSS 123540.19+123620.7	3.215	51.2 ± 9.5	(1)	9.370 ± 0.183			−0.612 ± 0.183
SDSS 123743.08+630144.8	3.425	7.7 ± 1.1	(1)	8.983 ± 0.901	< −1.55	(3)	0.119 ± 0.901
SDSS 124204.28+625712.1	3.321	8.6 ± 1.5	(1)	8.708 ± 1.029			0.079 ± 1.029
SDSS 124745.39+325147.0	2.249	≤4.4		9.208 ± 0.363			−0.444 ± 0.364
SDSS 125306.73+130604.9	3.624	10.8 ± 1.5		9.949 ± 0.112			−0.670 ± 0.113
SDSS 125319.10+454152.8	3.435	≤14.0		10.139 ± 0.492			−1.397 ± 0.493
SDSS 130216.13+003032.1	4.506	≤1.0	(2)		−2.08	(3)	
SDSS 131429.00+494149.0	3.813	13.9 ± 1.1	(1)	10.221 ± 0.134			−1.040 ± 0.135
SDSS 132603.00+295758.1	3.767	6.0 ± 0.5	(1)	9.802 ± 0.309			−0.434 ± 0.309
SDSS 132703.26+341321.7	2.558	6.6 ± 1.3		9.512 ± 0.562			−0.609 ± 0.562
SDSS 133146.20+483826.5	3.742	20.5 ± 3.6		9.949 ± 0.142			−0.803 ± 0.142
SDSS 133422.63+475033.5	4.950	≤6.9	(2)		−1.70	(3)	
SDSS 134521.39+281822.2	4.082	≤17.8		10.141 ± 0.700			−1.290 ± 0.701
SDSS 140300.23+432805.4	4.696	≤25.9		9.856 ± 0.943			−0.768 ± 0.943
SDSS 140850.91+020522.7	4.007	≤3.2			−1.54	(4)	

Table 1 – *continued*

Name	$z_{\rm SDSS}$	EW(C IV) (Å)	Ref.	$\log M_{\rm BH}$ ($M_{\odot}$)	$\alpha_{\rm ox}$	Ref.	$\log L_{\rm Bol}/L_{\rm Edd}$
SDSS 141209.96+062406.9	4.466	≤12.7		9.859 ± 1.217			−0.708 ± 1.218
SDSS 141318.86+450523.0	3.113	45.0 ± 5.4		9.095 ± 0.095			−0.202 ± 0.096
SDSS 141657.93+123431.6	2.603	≤3.9		9.159 ± 0.793			−0.126 ± 0.793
SDSS 142103.83+343332.0	4.907	≤50.5		9.841 ± 0.480	−2.07	(3)	−0.362 ± 0.481
SDSS 142144.98+351315.4	4.556	39.8 ± 5.9		9.884 ± 0.351			−0.531 ± 0.351
SDSS 142257.67+375807.4	3.163	39.5 ± 1.8	(1)	9.293 ± 0.609			−0.560 ± 0.610
SDSS 144127.65+475048.7	3.190	24.9 ± 1.9		8.598 ± 1.069			0.466 ± 1.069
SDSS 144231.71+011055.3	4.507	≤22.5			−1.42	(4)	
SDSS 144803.36+240704.2	3.544	≤12.5		9.967 ± 0.209			−0.905 ± 0.210
SDSS 155645.30+380752.8	3.320	≤2.4		8.407 ± 1.114			0.536 ± 1.115
SDSS 160336.64+350824.3	4.460	12.9 ± 2.3		10.296 ± 0.102			−0.820 ± 0.102
SDSS 161122.45+414409.5	3.131	19.6 ± 2.4		9.940 ± 0.165			−0.829 ± 0.166
SDSS 163411.82+215325.0	4.529	≤29.3		10.681 ± 0.221			−1.248 ± 0.221
SDSS 170108.89+395443.0	1.889	≤3.9		8.516 ± 0.568	−1.27	(5)	−0.056 ± 0.568
SDSS 210216.52+104906.6	4.182	16.6 ± 1.0	(1)	10.126 ± 0.440			−0.817 ± 0.441
SDSS 214753.29−073031.3	3.153	6.5 ± 0.8	(1)	9.786 ± 0.638			−0.868 ± 0.638
SDSS 223827.17+135432.6	3.516	28.5 ± 3.4		9.868 ± 0.121			−0.923 ± 0.122
SDSS 225246.43+142525.8	4.904	≤18.6		9.786 ± 0.340			−0.704 ± 0.341
SDSS 233255.72+141916.3	4.754	≤45.1		8.665 ± 1.053			0.009 ± 1.055
SDSS 233446.40−090812.2	3.317	10.4 ± 1.2		10.143 ± 0.110			−0.571 ± 0.110
SDSS 233939.48−103539.3	2.757	≤5.2		9.837 ± 0.525			−0.719 ± 0.525

Column (1) lists the object name. Column (2) shows the redshift taken from the SDSS DR7 quasar catalogue (Shen et al. 2011). Columns (3), (5) and (8) list the rest-frame EW of C IV emission line, logarithm of black hole mass and accretion rates in the Eddington units, respectively. Column (6) refers to the X-ray to optical luminosity ratio. The values without reference were taken from the SDSS DR7 quasar catalogue. A few EW(C IV) and all $\alpha_{\rm ox}$ values were taken from articles with references shown in columns (4) and (7). Numbers in parentheses correspond to the following references: (1) – Diamond-Stanic et al. (2009), (2) – this paper, (3) – Shemmer et al. (2009), (4) – Shemmer et al. (2006), (5) – Green et al. (2009).

However, we must note that there is a large spread in distribution of normal quasars around the linear fit. If we assume that a natural spread is less than 9 Å and we calculate the fit avoiding outliers, then the reduced χ^2 decreases to $\simeq$1.3. The estimated $\widetilde{\chi}^2$ for WLQs are $\sim$1000 and 2100 including and excluding upper limits on EW, respectively. The obtained values corroborate the hypothesis about difference in relationships.

We must keep in mind that $L_{\rm Bol}/L_{\rm Edd}$ values are calculated using the method based on the luminosity–$M_{\rm BH}$ relation, i.e. $L_{\rm Bol}/L_{\rm Edd} \propto$ FWHM (C IV)$^{-2}$. In many cases, the emission lines in WLQ objects are broad and their FWHM is equal to a few thousand km s^{-1} [see Mg II in Hryniewicz et al. (2010), Hβ in Shemmer et al. (2010) or C IV in Shen et al. (2011)]. Nevertheless, for weak C IV line (e.g. EW $<$ a few Å), the FWHM value is underestimated, and thus $L_{\rm Bol}/L_{\rm Edd}$ ratio is overestimated.

The existence of normal accretion rates in WLQs was discussed recently by Hryniewicz et al. (2010). They have argued that when the Eddington ratio increases, the widths of Lyα and Mg II lines decrease, C IV emission decreases; however, the Si IV line should become stronger, and the UV Fe II emission decreases. As the last two behaviours are not observed in WLQ (see e.g. Schneider et al. 2010),[5] Hryniewicz et al. (2010) claimed that the weakness of the emission lines in WLQs is not caused by high $L_{\rm Bol}/L_{\rm Edd}$.

So far, no observations of the FUV spectra of WLQs were made. Therefore, we analysed $\alpha_{\rm ox}$ which can shed light on the shapes of the SED in the FUV/soft X-ray band (Fig. 3). Apart from the spectral indices for WLQs, we analysed together with them 155 normal quasars. Their $\alpha_{\rm ox}$ values were taken from the *Chandra* Multiwavelength Project (Green et al. 2009). We cross-correlated this catalogue with SDSS DR7 quasar catalogue (Shen et al. 2011) to obtain the EW(C IV) of quasars. The solid line in Fig. 3 represents the best fit made by Wu et al. (2009). We must note that this linear fit was made to another sample of quasars; however, it fits very well to our sample of normal quasars. Our study clearly shows that $\alpha_{\rm ox}$ values in weak WLQs span the same region as seen in non-BAL and BAL QSOs. It points out that the UV/soft X-ray SED of WLQs is similar to those seen in normal AGNs and proves that a soft ionizing continuum is not the reason for the weakness of the lines. This situation is found in PHL 1811 which is NLS1 galaxy with super-Eddington rate ($L_{\rm Bol}/L_{\rm Edd} \sim$ 0.9–1.6) and steep ionizing continuum ($\alpha_{\rm ox} = -2.3$) (Leighly et al. 2007b). Therefore, PHL 1811 follows the relationship estimated by Wu et al. (2009).

4 DISCUSSION

The WLQs are shifted vertically in the log EW(C IV)–log $L_{\rm Bol}/L_{\rm Edd}$ plane relative to normal quasars (Fig. 2). This offset and the fact that QSOs and WLQs SED are almost the same indicate that weak WLQs are normal AGNs, however, with intrinsically weak C IV emission line. It is also clearly shown that the super-Eddington luminosities are not required in weak-line quasars, contrasting with the idea that WLQs are super-Eddington sources (Leighly et al. 2007b). Furthermore, the accretion rates in WLQs span the same interval as normal quasars (Fig. 2).

[5] http://www.sdss.org/dr7/

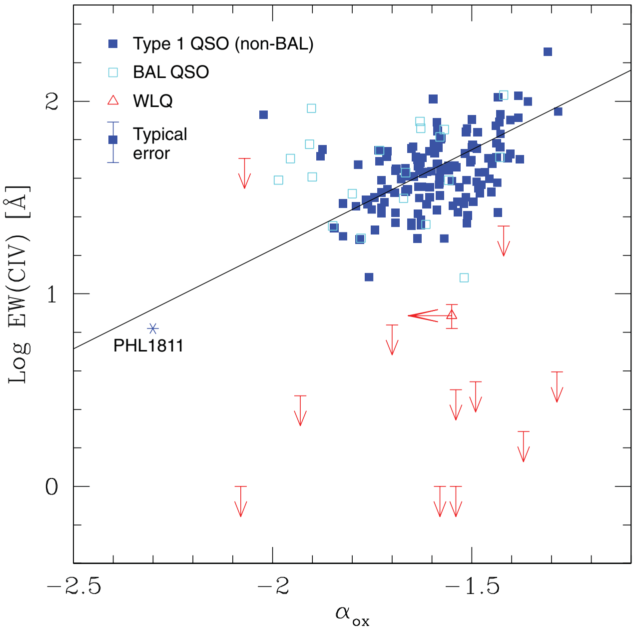

Figure 3. Rest-frame EW of C IV emission line versus spectral index $\alpha_{\rm ox}$. Solid blue and open cyan squares refer to type 1 non-BAL and BAL quasars, respectively. The 155 radio-quiet and radio-intermediate sources are taken from Green et al. (2009). Solid red triangles and upper limits show 12 WLQ objects. Star denotes NLS1 PHL 1811. Solid line is the relationship obtained by Wu et al. (2009). Typical error of non-BAL and BAL QSOs is shown in the legend.

The SEDs of weak-line quasars observed in optical/UV band (till $\sim$ 1200 Å) do not differ from the SEDs of normal quasars (e.g. Diamond-Stanic et al. 2009). However, the FUV spectrum of AGNs and their relative quietness in the soft X-ray band produce weak emission lines as supported by photoionization modelling (see e.g. Leighly 2004; Leighly & Casebeer 2007, for review). Due to the absence of the FUV spectra of WLQs, we analysed the X-ray to optical luminosity ratio $\alpha_{\rm ox}$ of different quasars (Fig. 3). Similar analysis was carried out by Richards et al. (2011, see their fig. 9) and Wu et al. (2011, see their fig. 6). We focus on weak WLQs and enlarged our sample by adding objects with log EW(C IV) < 0.6. Our analysis indicates that the UV/soft X-ray SED of WLQs is similar to those of normal AGNs and a soft ionizing continuum is not the reason for the weakness of the lines.

The intensity of an emission line depends on the flux of ionizing continuum, $L_{\rm ionize}$, and on the BLR gas covering factor, $\Omega/4\pi$: $L(\rm line) \sim L_{\rm ionize} \times \Omega/4\pi$ (see Ferland 2004, and his discussion for He II λ1640). The spectral index, $\alpha_{\rm ox}$, measures by definition the ratio of the luminosities at 2 keV to those at 2500 Å. If we assume that $L_\nu(2500\,\text{Å})$ is roughly equal to $L_\nu(1450\,\text{Å})$ and assuming that $L_\nu(2\,\rm keV) \simeq L_{\rm ionize}$, we can write $\alpha_{\rm ox} \sim \log L_{\rm ionize} - \log L_\nu(1450\,\text{Å})$. We can then express the line EW as

$$\log {\rm EW(line)} \approx {\rm const}_1 + \log \frac{\Omega}{4\pi} + \frac{\alpha_{\rm ox}}{{\rm const}_2}.$$

The correlation EW(C IV)–$\alpha_{\rm ox}$ obtained for normal quasars by e.g. Wu et al. (2009) infers that the gas covering factor in BLR in type 1 quasars is relatively constant. The gas covering factor in WLQ objects behaves differently (Fig. 3), suggesting that $\Omega_{\rm WLQ}$ is $\gtrsim$10 times smaller than in QSOs.

Table 2 compares the emission-line intensity ratios observed in Seyfert 1.5 galaxy NGC 5548, normal quasars and WLQs. We focus on 59 'real WLQs', i.e. our selected subsample which consists of sources with EW(C IV) $\lesssim$ 20 Å and EW(Lyα) < 15.4 Å (see column 7 of Table 2). We take into account line intensities produced by HILs (such as Lyα, C IV), intermediate-ionization lines (IILs; e.g. C III]) and low-ionization lines (LILs; such as Mg II, Hβ). The C IV/Lyα intensity ratios for different sources are the same from a statistical point of view. The ratios between the covering factors of the regions responsible for producing C IV and Lyα are therefore similar in WLQs and QSOs. Comparing LILs and IILs with HILs, we obtain that the ratios of the covering factors of HIL/LIL and IIL/LIL are lower in WLQs that in normal quasars, even if for WLQ these ratios are based on only few sources. This suggests that the covering factor of the BLR is smaller in WLQ.

This is in agreement with observations of the weak Hβ emission lines in SDSS J114153.34+021924.3 and SDSS J123743.08+630144.9 (Shemmer et al. 2010). There the authors have explained the weakness of their emission lines by a deficit of the BLR. The absence of BLR in WLQs has also been recently suggested by Liu & Zhang (2011). The existence of bright AGNs with dusty tori, but without BLR, could be understood when an anisotropic radiative pressure is released from an accretion disc. Liu & Zhang stated that this is possible just before the normal phase of an AGN. Additionally, Leighly & Moore (2004) suggested based on observations of the emission-line profiles of NLS1 galaxies IRAS 13224−3809 and 1H 0707−495 that the HILs are produced in a wind and that the IILs and LILs are produced in low-velocity gas associated with the accretion disc at the base of the wind. Both pictures are consistent with a suggestion that the regions producing emission lines are developed by winds (Hawkins 2004; Hryniewicz et al. 2010). In that case, when the BLR is created, its covering factor is lower than estimated in normal AGNs.

There is an observational analogy between weak WLQs and the class of 'optical dull' AGNs [also called 'X-ray bright, optically normal galaxies' (XBONGs)]. Their X-ray emission is bright, while they lack both the broad emission lines of type 1 AGNs and the narrow emission lines of type 2 AGNs (Elvis et al. 1981; Comastri et al. 2002; Georgantopoulos & Georgakakis 2005). There are a few hypotheses trying to answer the latent nature of XBONGs (see e.g. Moran, Filippenko & Chornock 2002; Severgnini et al. 2003; Rigby et al. 2006; Civano et al. 2007; Trump et al. 2009). However, none of them (such as dilution of their spectra by a host galaxy, the low Eddington accretion rate) can explain WLQs.

Elvis (2000) has proposed an empirically derived structure for quasars. He suggests the presence of funnel-shaped geometrically thin accretion outflow which contains an high-ionized gas embedded in the colder BLR clouds. According to our paper, the low covering factor of the BLR means that WLQ has got less clouds in the outflow or equivalently the 'funnel' wind is geometrically thinner.

Low covering factor of the BLR in WLQs would have additional consequence observed in the infrared (IR) band. Gaskell et al. (2007) have argued that the covering factors of the BLR and of the dusty torus have to be the same. It means that a small BLR in WLQs causes an evaporation of dust in the torus and a reduction of its IR emissivity. Diamond-Stanic et al. (2009) mentioned that two weak-line quasars SDSS J140850.91+020522.7 [with EW(C IV) = 1.95 Å] and SDSS J144231.72+011055.2 [with EW(C IV) = 16.9 Å] are fainter in the IR ($\sim$24 μm) band by 30–40 per cent. Additionally, the IR flux density of SDSS J130216.13+003032.1 [EW(C IV) = 27.8 Å] is also relatively low. More IR observations of WLQs are required to confirm this hypothesis.

Table 2. Arithmetic means and standard deviations of the emission-line intensity ratios. All observed line fluxes were dereddened for the Milky Way contamination.

Ratio	NGC 5548		PG QSO	Non-BAL QSO	BAL QSO	WLQ(all)	WLQ(sub)
(1)	(2a)	(2b)	(3)	(4)	(5)	(6)	(7)
C IV/Lyα	1.45	0.94	0.46 ± 0.14			1.62 ± 1.57	0.59 ± 0.42^a
C IV/Mg II	5.80	4.98	4.38 ± 1.54	3.36 ± 1.47	3.03 ± 1.34		0.44 ± 0.21^b
C III](λ1909)/Mg II	1.07	0.91	0.99 ± 0.20				0.16 ± 0.02^c
Lyα/Hβ	8.57		11.75 ± 3.25				1.81 ± 0.17^d

Column (1) refers to the names of intensity ratios. In the case of Seyfert 1.5 galaxy NGC 5548, those values are shown in columns (2a) and (2b). In column (2a), the Lyα, C IV and C III] fluxes are taken from Korista et al. (1995), the Mg II flux from Gaskell, Klimek & Nazarova (2007), and the Hβ flux from Wanders & Peterson (1996). The ratios in column (2b) are calculated from corrected for narrow-line fluxes and taken from Korista & Goad (2000). Column (3) refers to sample of 18 radio-quiet PG quasars (Shang et al. 2007). Values of intensity ratio of radio-quiet and radio-intermediate 97 non-BAL and 14 BAL quasars are shown in columns (4) and (5), respectively. These sources were selected after cross-matching SDSS DR7 quasar catalogue (Shen et al. 2011) with Green et al. (2009) sample. This sample is consistent with the sample used in Fig. 3. In column (6), we calculate mean ratio for all WLQs which show weak or strong C IV lines. Column (7) refers to subsample of WLQs, for which EW(C IV) < 20 Å and EW(Lyα) < 15.4 Å.
[a]Mean is calculated from 59 WLQs; [b]mean from SDSS J094534 and SDSS J170109; [c]value only for SDSS J094534; [d]mean from SDSS J114153.34+021924.3 and SDSS J123743.08+630144.9.
Data for intensity of C IV line in WLQs are taken from Shen et al. (2011), for Lyα from Diamond-Stanic et al. (2009), for C IV/Mg II and C III]/Mg II ratios from Hryniewicz et al. (2010) and Hryniewicz et al. (in preparation), and for Hβ from Shemmer et al. (2010).

5 CONCLUSIONS

We have explored the BEff in 82 high-redshift ($z > 2.2$) and two intermediate-redshift weak-line quasars (WLQ) and compared them with a set of normal quasars. We draw the following conclusions.

(i) The relationship between the rest-frame EW for C IV emission line and the Eddington ratio observed in WLQs has different normalization than for normal QSOs. This shift disagrees with the super-Eddington hypothesis (e.g. Shemmer et al. 2010).

(ii) The weakness or even the absence of emission lines in WLQs is likely caused by a low covering factor of the BLR rather than by a very soft ionizing continuum. The comparison of the EW(C IV) and the spectral indices, $\alpha_{\rm ox}$, shows that the gas covering factor of the BLR in WLQs is $\gtrsim$10 times less than for normal QSOs.

(iii) The ratios of the covering factors of regions responsible for producing C IV and Lyα are similar in WLQs and QSOs.

(iv) The ratios of the covering factors $\Omega_{\rm HIL}/\Omega_{\rm LIL}$ are lower in WLQ than in QSOs, showing the deficit of the BLR in WLQ. However, this result is based on observations of only four sources.

(v) The radio-intermediate quasar SDSS J170109 ($z = 1.89$) is a new intermediate-redshifted WLQ with rest-frame EW(C IV) = 2.09 Å and EW(Mg II) = 9.41 Å (Shen et al. 2011).

(vi) The definition of WLQ objects should take into account the weakness of Lyα or C IV emission lines not only separately, but also together. 'False WLQs' (sources with prominent C IV) are probably normal type 1 quasars with intervening Lyα absorption.

ACKNOWLEDGMENTS

We would like to thank an anonymous referee for useful comments that improve our paper. We are grateful to Bozena Czerny, Krzysztof Hryniewicz and Joanna Kuraszkiewicz for advices during calculation and analysis. We also thank Gary Ferland for pointing out a helpful article. MN thanks the Scientific Exchange Programme (Sciex) NMS[ch] for the opportunity of working at the ISDC. This research has been supported in part by the Polish MNiSW grants NN203 380136 and 362/1/N-INTEGRAL/2008/09/0.

REFERENCES

Anderson S. F. et al., 2001, AJ, 122, 503
Avni Y., Tananbaum H., 1982, ApJ, 262, L17
Bachev R., Marziani P., Sulentic J. W., Zamanov R., Calvani M., Dultzin-Hacyan D., 2004, ApJ, 617, 171
Baldwin J. A., 1977, ApJ, 214, 679
Baskin A., Laor A., 2004, MNRAS, 350, L31
Baskin A., Laor A., 2005, MNRAS, 356, 1029
Bianchi S., Guainazzi M., Matt G., Fonseca Bonilla N., 2007, A&A, 467, L19
Boroson T. A., Green R. F., 1992, ApJS, 80, 109
Cardelli J. A., Clayton G. C., Mathis J. S., 1989, ApJ, 345, 245
Civano F. et al., 2007, A&A, 476, 1223
Collinge M. J. et al., 2005, AJ, 129, 2542
Comastri A. et al., 2002, ApJ, 571, 771
Diamond-Stanic A. M. et al., 2009, ApJ, 699, 782
Dietrich M., Hamann F., Shields J. C., Constantin A., Vestergaard M., Chaffee F., Foltz C. B., Junkkarinen V. T., 2002, ApJ, 581, 912
Dong X., Wang J., Wang T., Wang H., Fan X., Zhou H., Yuan W., Long Q., 2009, in Wang W., Yang Z., Luo Z., Chen Z., eds, ASP Conf. Ser. Vol. 408, The Starburst-AGN Connection. Astron. Soc. Pac., San Francisco, p. 83
Elvis M., 2000, ApJ, 545, 63
Elvis M., Schreier E. J., Tonry J., Davis M., Huchra J. P., 1981, ApJ, 246, 20
Fan X. et al., 1999, ApJ, 526, L57
Fan X. et al., 2006, AJ, 131, 1203
Ferland G., 2004, in Richards G. T., Hall P. B., eds, ASP Conf. Ser. Vol. 311, AGN Physics with the Sloan Digital Sky Survey. Astron. Soc. Pac., San Francisco, p. 161
Fine S., Croom S. M., Bland-Hawthorn J., Pimbblet K. A., Ross N. P., Schneider D. P., Shanks T., 2010, MNRAS, 409, 591
Gaskell C. M., Klimek E. S., Nazarova L. S., 2007, preprint (arXiv: 0711.1025)
Georgantopoulos I., Georgakakis A., 2005, MNRAS, 358, 131
Gibson R. R., Brandt W. N., Schneider D. P., 2008, ApJ, 685, 773
Gilbert K. M., Peterson B. M., 2003, ApJ, 587, 123
Green P. J., Forster K., Kuraszkiewicz J., 2001, ApJ, 556, 727
Green P. J. et al., 2009, ApJ, 690, 644
Hawkins M. R. S., 2004, A&A, 424, 519

Hryniewicz K., Czerny B., Nikołajuk M., Kuraszkiewicz J., 2010, MNRAS, 404, 2028
Iwasawa K., Taniguchi Y., 1993, ApJ, 413, L15
Jiang P., Wang J. X., Wang T. G., 2006, ApJ, 644, 725
Jiang L., Fan X., Ivezić Ž., Richards G. T., Schneider D. P., Strauss M. A., Kelly B. C., 2007, ApJ, 656, 680
Just D. W., Brandt W. N., Shemmer O., Steffen A. T., Schneider D. P., Chartas G., Garmire G. P., 2007, ApJ, 665, 1004
Keremedjiev M., Hao L., Charmandaris V., 2009, ApJ, 690, 1105
Kinney A. L., Rivolo A. R., Koratkar A. P., 1990, ApJ, 357, 338
Kong M., Wu X., Wang R., Liu F. K., Han J. L., 2006, A&A, 456, 473
Korista K. T., Goad M. R., 2000, ApJ, 536, 284
Korista K. T. et al., 1995, ApJS, 97, 285
Korista K., Baldwin J., Ferland G., 1998, ApJ, 507, 24
Kuraszkiewicz J. K., Green P. J., Forster K., Aldcroft T. L., Evans I. N., Koratkar A., 2002, ApJS, 143, 257
Laor A., 1998, ApJ, 505, L83
Laor A., Fiore F., Elvis M., Wilkes B. J., McDowell J. C., 1997, ApJ, 477, 93
Leighly K. M., 2004, ApJ, 611, 125
Leighly K. M., Casebeer D., 2007, in Ho L. C., Wang J.-W., eds, ASP Conf. Ser. Vol. 373, The Central Engine of Active Galactic Nuclei. Astron. Soc. Pac., San Francisco, p. 365
Leighly K. M., Moore J. R., 2004, ApJ, 611, 107
Leighly K. M., Halpern J. P., Jenkins E. B., Casebeer D., 2007a, ApJS, 173, 1
Leighly K. M., Halpern J. P., Jenkins E. B., Grupe D., Choi J., Prescott K. B., 2007b, ApJ, 663, 103
Liu Y., Zhang S. N., 2011, ApJ, 728, L44
McDowell J. C., Canizares C., Elvis M., Lawrence A., Markoff S., Mathur S., Wilkes B. J., 1995, ApJ, 450, 585
Moran E. C., Filippenko A. V., Chornock R., 2002, ApJ, 579, L71
Netzer H., Laor A., Gondhalekar P. M., 1992, MNRAS, 254, 15
Plotkin R. M. et al., 2010a, AJ, 139, 390
Plotkin R. M., Anderson S. F., Brandt W. N., Diamond-Stanic A. M., Fan X., MacLeod C. L., Schneider D. P., Shemmer O., 2010b, ApJ, 721, 562
Pogge R. W., Peterson B. M., 1992, AJ, 103, 1084
Richards G. T. et al., 2003, AJ, 126, 1131
Richards G. T. et al., 2011, AJ, 141, 167
Rigby J. R., Rieke G. H., Donley J. L., Alonso-Herrero A., Pérez-González P. G., 2006, ApJ, 645, 115
Risaliti G., Young M., Elvis M., 2009, ApJ, 700, L6
Schneider D. P. et al., 2003, AJ, 126, 2579
Schneider D. P. et al., 2005, AJ, 130, 367
Schneider D. P. et al., 2007, AJ, 134, 102
Schneider D. P. et al., 2010, VizieR Online Data Catalog, 7260, 0
Severgnini P. et al., 2003, A&A, 406, 483
Shang Z., Wills B. J., Robinson E. L., Wills D., Laor A., Xie B., Yuan J., 2003, ApJ, 586, 52
Shang Z., Wills B. J., Wills D., Brotherton M. S., 2007, AJ, 134, 294
Shemmer O. et al., 2006, ApJ, 644, 86
Shemmer O., Brandt W. N., Anderson S. F., Diamond-Stanic A. M., Fan X., Richards G. T., Schneider D. P., Strauss M. A., 2009, ApJ, 696, 580
Shemmer O. et al., 2010, ApJ, 722, L152
Shen Y. et al., 2011, ApJS, 194, 45
Shields J. C., 2007, in Ho L. C., Wang J.-W., eds, ASP Conf. Ser. Vol. 373, The Central Engine of Active Galactic Nuclei. Astron. Soc. Pac., San Francisco, p. 355
Strateva I. V., Brandt W. N., Schneider D. P., Vanden Berk D. G., Vignali C., 2005, AJ, 130, 387
Trump J. R. et al., 2009, ApJ, 706, 797
Vestergaard M., Peterson B. M., 2006, ApJ, 641, 689
Wanders I., Peterson B. M., 1996, ApJ, 466, 174
Warner C., Hamann F., Dietrich M., 2004, ApJ, 608, 136
Wu J., Vanden Berk D. E., Brandt W. N., Schneider D. P., Gibson R. R., Wu J., 2009, ApJ, 702, 767
Wu J. et al., 2011, ApJ, 736, 28
Xu Y., Bian W., Yuan Q., Huang K., 2008, MNRAS, 389, 1703
Zamorani G., Marano B., Mignoli M., Zitelli V., Boyle B. J., 1992, MNRAS, 256, 238
Zhou X., Wang J., 2005, ApJ, 618, L83

This paper has been typeset from a TEX/LATEX file prepared by the author.